Available online www.jocpr.com

Journal of Chemical and Pharmaceutical Research, 2015, 7(5):793-797

Research Article

ISSN : 0975-7384
CODEN(USA) : JCPRC5

Copper phosphate nanoparticles: Synthesis, characterisation and their antibacterial activity

S. Ramesh, K. Giribabu, S. Praveen Kumar, R. Manigandan and V. Narayanan*

Department of Inorganic Chemistry, University of Madras, Guindy Campus, Chennai, India

---

ABSTRACT

Copper phosphate nanoparticles were synthesized by simple precipitation method. The crystalline nature of the sample was confirmed by X-ray diffraction (XRD). FT-IR establishes the formation of the copper phosphate. The DRS-UV spectrum showed bands corresponding to tetragonal distortion in the coordination sphere around Cu^{2+}. The morphology (layered flakes) and size (50 to 55 nm) was verified by TEM analysis. Copper phosphate nanoparticles were screened for antimicrobial activities against two gram positive bacteria and two gram negative bacteria. The bioactive assay showed that copper phosphate exhibited moderate to good antimicrobial activities against gram positive - staphylococcus aureus (SA), bacillus cereus (BA) and gram negative - E.coli (BB), salmonella (BC) bacteria.

Key words: Copper phosphate, *Staphylococcus aureus (SA), Bacillus cereus (BA), E.coli (BB), Salmonella (BC).*

INTRODUCTION

In the recent methods, many antibacterial agents that has metal atoms or ions such as copper and zinc have been developed [1]. Inorganic antibacterial agents has better properties like long-lasting effects, broad-spectrum antibiotics and better heat resistance which will be helpful for the synthesis of antibacterial materials. copper ion is well known for its good antibacterial activity and low toxicity compared with many other metal ions [2,3]. From ancient times phosphate containing molecules/compounds has been used for the healing of burns, wounds, dental work and various bacterial infections [4]. After the invasion of antibiotics, the applications of silver compounds in the medicinal field have lost its importance slowly. Presently, nanotechnology plays a vital role in reducing the bulk metal size into their nanosize and drastically enhances the unique physicochemical characteristics such as catalytic activity, optical properties, electronic properties, antimicrobial activity, and magnetic properties [5]. So silver has made a re-entry as an antimicrobial agent in the form of nanoparticles. Several harmful bacteria became resistant to various antibiotics; hence the use of silver nanoparticles is gaining its importance. Many researchers suggested the use of silver and copper ions as a disinfectant for waste water containing harmful microorganism. But the metallic copper and silver ions in the water may affect the human's health. The antimicrobial property of metal nanoparticles is due to their reduced size and high surface to volume ratio which permits them to interact closely with microorganism membranes and is not merely due to the release of metal ions in solution. It was believed that heavy metals react with proteins by joining with thiol groups, which leads to the inactivation of the proteins[6].

The various bactericidal effects of copper nanoparticles are very well known and their mechanisms are explained. But very few research works are carried out to explain the copper nanoparticles antimicrobial property[7]. Yoon et al. studied the bactericidal effects of metal nanoparticles using single representative strains of E.Coli and Bacillus subtills and found that copper nanoparticles has superior antibacterial activity than the silver nanoparticles [8]. The present study deals with the antimicrobial property of copper phosphate nanoparticle using various microbial strains. The metal phosphate nanoparticles typically suggested for the use in antimicrobial assays i.e, gram positive [Staphylococcus aureus (SA), Bacillus cereus (BA)], Gram negative [E. coli (BB), Salmonella (BC)]. The

antimicrobial effect was quantified based on the inhibition zone measured in the disk diffusion tests conducted in plates and by determining the minimum growth inhibitory concentrations (MIC) in liquid batch cultures.

EXPERIMENTAL SECTION

Materials

Copper acetate, and silver acetate were purchased from Sigma-Aldrich. Phosphoric acid, acetone, hydrazine hydrate and ethanol were purchased from SRL India Ltd., and used as received. Double distilled water used as solvent throughout the experiment.

Synthesis of the copper phosphate nanoparticle

Copper phosphate nanoparticles were synthesized by reacting stoichiometric amount of copper acetate and phosphoric acid. 3 mmol of copper acetate was dissolved in 150 mL distilled water, which was homogenized for 20 min with stirring. After 20 min, 3 mmol of phosphoric acid was added slowly into the copper acetate solution. The colourless-cloudy precipitate was formed, after that 2 mL of hydrazine hydrate were also added to it. The resulting colourless foam-like product was centrifuged and washed with de-ionized water thrice. In addition, the product was precipitated by adding ethanol (20 mL) followed by two to three cycles of centrifugation at 4000 rpm to remove excess unreacted species. Then the precipitate is calcined at 300 ^{o}C for 24 hours. Similarly Ag-Cu_3PO_4 nanoparticles were prepared by taking 8 mmol of copper acetate and 8 mmol of o-phosphoric acid to form the colloidal solution. Then centrifuged, washed with distilled water and ethanol to remove any dissolved impurities.

Characterization

Crystal structure, crystallite size and lattice parameter of the product was determined by Rich Siefert 3000 diffractometer with Cu $K_{\alpha1}$ radiation (λ = 1.5406 Å). Fourier transform Infrared spectroscopy (FTIR) spectrum was recorded on a Perkin Elmer FTIR spectrophotometer in the region of 4000 to 400 cm^{-1}. The morphology was analyzed by HITACHI SU6600 (FE-SEM) field-emission scanning electron microscopy coupled with energy dispersive angle X-ray (EDAX) and high resolution transmission electron microscopy (HRTEM) using a FEI TECNAI G^2 model T-30 at accelerating voltage of 250 kV. Raman spectrum was recorded using laser confocal microscope, Raman-11 Nanophoton Corporation, Japan and diffused reflectance-ultraviolet-visible (DRS-UV-Vis) absorbance spectrum was recorded using Perkin Elmer lambda 650 spectrophotometer.

RESULTS AND DISCUSSION

XRD pattern of the as-synthesized copper phosphate nanoparticles were shown in Figure 1. All the diffraction peaks could be indexed to the monoclinic phase matched with standard card (JCPDS. No: 049-1145) of $Cu_4H(PO_4)_3.3H_2O$. For the sample calcined at 300 °C, the XRD pattern showed well defined diffraction peaks[9-13]. The peak broadening in the diffraction patterns is indicative of smaller crystallite size of 50 to 55 nm. The crystallite size of the copper phosphate nanoparticles were calculated using Scherer relation.

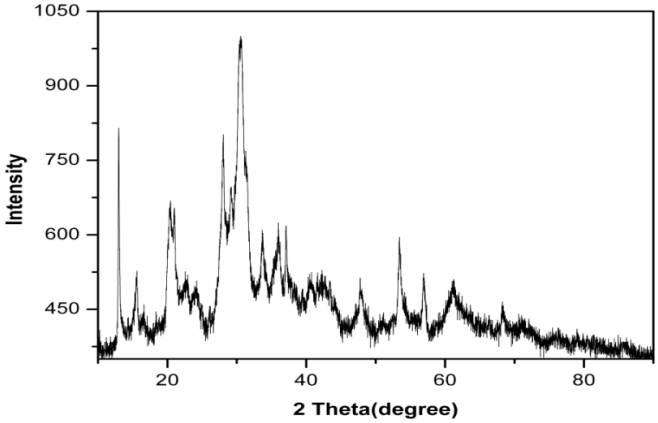

Figure 1: XRD pattern of $Cu_4H(PO_4)_3.3H_2O$

DRS- UV visible spectrum of copper phosphate is shown in Fig 2. The intense broad absorption band at 250 nm (λ_{max}) is due to electronic excitation in phosphate. The low energy absorption band extending from 550 nm to near IR region is due to electronic transition (d-d transition in Cu^{2+}). Such a broad absorbance is attributed to octahedral environment of phosphate around Cu^{2+}. It is expected tetragonal distortion for the coordination sphere. As a result of distortion the axial oxidic sites are to be far off compared to equatorial oxidic sites. As a result the doublet t_2g level of Cu^{2+} is split into doublet e_g (low energy orbitals) doublet b_2g orbital high energy state , doublet e_g level is split

into doublet a_1g(low energy) and doublet b_1g(high energy). For this splitting the expected d-d transitions are doublet $a_1g \rightarrow$ doublet b_1g. doublet $a_1g \rightarrow$doublet b_1g and doublet $e_g \rightarrow$ doublet b_1g as shown in figure 2a. As result of these three transitions the absorbance is broad. As a spectrum was UV vis region the three absorbance bands are not deconvulted in this spectrum. The appearance of green color is also due to the portion of absorbance occurring in the visible region[14].

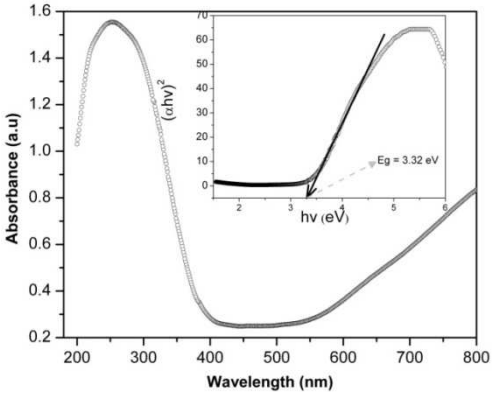

Figure 2: DRS-UV-Visible spectrum of $Cu_4H(PO_4)_3.3H_2O$

The FTIR spectrum of copper phosphate is shown in figure 3. The intense broad peak in the high energy region is due to O-H stretching vibration of water and phosphate. Presence of water in copper phosphate is confirmed by its bending vibration at about 1620 $cm^{-1.}$ As the OH stretching vibration showed a sudden fall in transmittance at about 3500 cm^{-1}.The phosphate ligand might have at least an OH group. The phosphate vibration yielded a very intense band at about 1000 cm^{-1}. The short peak around 550 cm^{-1} is ascribed to copper oxide vibration CuO[15]. So this IR spectrum evidently proves phosphate ligand with at least an -OH group and water molecules.

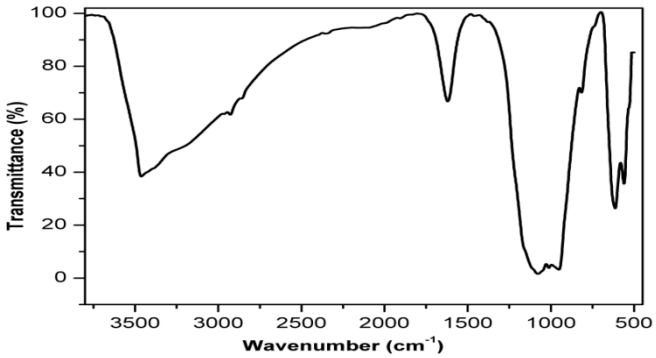

Figure 3: FTIR spectrum of $Cu_4H(PO_4)_3.3H_2O$

The Raman spectrum of copper phosphate is shown in figure 4. As the OH bond is very much polar their vibrations are not observed in the Raman spectrum[16]. The phosphate vibrations yielded peaks at about 1000 cm^{-1}. The group of peaks around 500 cm^{-1} is due to copper oxide vibrations.

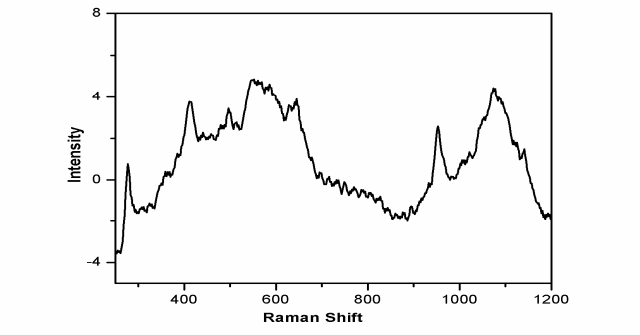

Figure 4: Raman spectra of $Cu_4H(PO_4)_3.3H_2O$

Figure 5a, and 5b shows the FESEM-EDAX images of the as prepared copper phosphate nanoparticles, which clearly indicates that the product consists of layered flakes. The high magnification FESEM image (Figure 5b) exhibits that the formation of flake shaped particle. The inspection of images suggests that the coalescence between the particles may contribute to the growth by the orientation mechanism in the precipitation method. In addition, the elemental analysis was obtained by EDAX analysis, shown in Figure 4c, which clearly demonstrates homogeneous distribution of copper, phosphorous, oxygen, and carbon elements. HRTEM images of copper phosphate nanoparticles shown in Figure 6a, 6b, 6c and 6d reveals that the observed results well-matched with the FESEM results. In agreement with the FE-SEM results, the average diameter was measured in the range of 50-55 nm. Selected area energy diffraction (SAED) pattern shown in Figure 6e reveals that the particles were highly crystalline in nature. The images represents of copper phosphate nanoparticles at 300 °C, reveals that the particles were close to elongated spheroids with aggregation due to the temperature. While magnifying image (Figure 6b) shows the bar like flakes. The growth of the plate like structure was confirmed by the HRTEM images which evidences the presence stacked flakes with little aggregation, and it was in good agreement with the FESEM-EDAX results shown above.

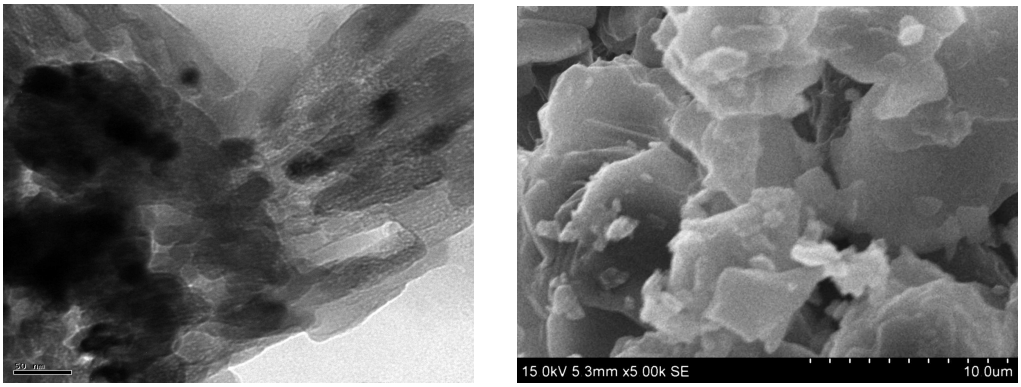

Figure 5: (a) FE SEM & (b)HRTEM image of $Cu_4H(PO_4)_3.3H_2O$

Figure 6: Digital photograph of antimicrobial activities for $Cu_4H(PO_4)_3.3H_2O$

Antibacterial assays

The antimicrobial activities of the test compounds and Streptomycin (Hi-media) were determined against gram positive and gram negative pathogens as described previously [17] . The Silver-copper phosphate nanocomposites were dissolved (10 mg/mL) in DMSO (Sigma) to provide stock solutions. A single colony of test strain was pre-grown overnight in 2 mL Muller–Hinton broth (MHB) at 37 C with constant shaking at 225 rpm. The following day, the inocula were prepared by diluting the overnight culture with 0.9% NaCl to a 0.5 McFarland standard. The agar diffusion method was followed for antibacterial susceptibility test. Petri plates were prepared by pouring 19 ml of Mueller Hinton Agar and allowed to solidify. These agar plates were inoculated with 0.1 ml of standardized bacterial suspension ($2x10^6$cells/ml) and uniformly spread. A 6 mm well was cut at the centre of the agar plate and the well was loaded with 100**µl** of each test compound (dissolved in DMSO). The diameter of the inhibition zone observed around the well was measured for each bacterium after 24 hrs of incubation at 37° C. The well filled with DMSO served as negative control and the well filled with Streptomycin served as a positive control. In an era of

antibiotic resistance the pathogens can be challenged cleverly with metallic nanoparticles as their complex mechanism of action on different bacterial structures, gives them an advantage when compared to the available antibiotics. Kon. K, and Rai. M (2013). Copper phosphate nanoparticles showed activity against both gram +ve and gram –ve pathogens. This suggest that these Silver-copper phosphate nanoparticles have higher affinity towards the cell wall of the gram +ve pathogen comparatively compounds 8 has higher affinity towards gram –ve cell wall.

CONCLUSION

A simple method has developed to synthesize silver doped copper phosphate nanoparticles by simple precipitation method. The same precipitation method could also be applied for the synthesis of other silver doped heavy metal phosphates. As silver doper copper phosphate nanoparticles showed activity against gram positive and gram negative bacteria, the silver doped other heavy metal phosphates could also be expected to have such activity. We believe that our method has a number of advantages including the simple reaction conditions, environmental friendly, and high reproducibility.

.**Acknowledgement**
The author acknowledges the Department of Nanoscience and Nanotechnology for providing support like FE-SEM, HRTEM, DRS-UV-Vis and Raman facilities.

REFERENCES

[1] AM Mulligan;M Wilson; JC Knowles; *Biomaterials*., **2003**, 24(10), 1797–1807.
[2] G Grass C. Rensing; M. Solioz, *Appl. Environ. Microb*., **2011**, 77(5), 1541–1547.
[3] M Ibrahim; F Wang; M Lou; G. Xie; B. Li; Z. Bo; G. Zhang; H. Liu; A. Wareth, *J.Biosci. Bioeng*., **2011**, 112(6), 570–576.
[4] A Akashi; Y Matsuya; M Unemori; A Akamine, *Biomaterials*., **2001**, 22(20),2713-7.
[5] D Laha; D Bhattacharya; A Pramanik; CR Santra; P Pramanik; P Karmakar, *Toxicol. Res*., **2012**, 1, 131-136.
[6] S JS Flora, *Oxid Med Cell Longev.*, **2009**, 2(4), 191–206.
[7] GC Leite; MC Padoveze, J. Infect Control., **2012**, 1(2), 33-36.
[8] U Kalinowska-Lis; EM Szewczyk; L Chęcińska; JM Wojciechowski; WM Wolf; J Ochocki, *ChemMedChem.*, **2014**, 9(1), 169–176.
[9] H Onoda; K Okumoto; A Nakahira; I Tanaka, *Materials*., **2009**, 2, 1-9.
[10] H Onoda; K Okumoto, *Materials Sciences and Applications*., **2011**, 209-214.
[11] J Koo; B Bae; H Na, *J. Non-Cryst. Solids.*, **1997**,212(2–3), 173–179.
[12] CE Bamberger; ED Specht; LM Anovitz, *J. Am. Ceram. Soc.*, **1997**,80 (12), 3133–38.
[13] N Khan; VA Morozov; SS Khasanov; BI Lazoryak, *Mater. Res. Bull*., **1997**, 32(9), 1211–1220.
[14] SK Verma;RR Yadav, *Platin Met Rev.*, **2013**, 57(3), 186.
[15] FA Miller; CH Wilkins, *Anal Chem*., **1952**, 24, 1294.
[16] J Koo; BS Bae; HK Na, *J Non-Cryst Solids*., **1997**, 212, 173 – 179.
[17] I Sondi; BS Sondi, *J Colloid Interf Sci*., **2004**, 275, 177–182.